PNAS RESEARCH ARTICLE | BIOCHEMISTRY

Elevated intracellular Na^+ and osmolarity stimulate catalytic activity of the ubiquitin ligase Nedd4-2

Avinash Persaud[a], Chong Jiang[a], Zetao Liu[a,b], George Kefalas[a,b], Wael L. Demian[a,b], and Daniela Rotin[a,b,1]

Edited by Aaron Ciechanover, Technion Israel Institute of Technology, Ruth and Bruce Rappaport Faculty of Medicine, Bat Galim, Haifa, Israel; received December 16, 2021; accepted May 26, 2022

Regulation of catalytic activity of E3 ubiquitin ligases is critical for their cellular functions. We identified an unexpected mode of regulation of E3 catalytic activity by ions and osmolarity; enzymatic activity of the HECT family E3 Nedd4-2/Nedd4L is enhanced by increased intracellular Na^+ ($[Na^+]_i$) and by hyperosmolarity. This stimulated activity is mediated by activation of p38-MAPK and is inhibited by WNKs. Moreover, protease (Furin)–mediated activation of the epithelial Na^+ channel ENaC (a bona fide Nedd4-2 substrate), which leads to increased $[Na^+]_i$ and osmolarity, results in enhanced Nedd4-2 catalytic activity. This enhancement is inhibited by a Furin inhibitor, by a protease-resistant ENaC mutant, or by treatment with the ENaC inhibitor amiloride. Moreover, WNK inhibition, which stimulates catalytic activity of Nedd4-2, leads to reduced levels of cell-surface ENaC and reduced channel activity. ENaC activity does not affect Nedd4-2:ENaC binding. Therefore, these results demonstrate activation of a ubiquitin ligase by Na^+ and osmotic changes. Importantly, they reveal a negative feedback loop in which active ENaC leads to stimulation of catalytic activity of its own suppressor, Nedd4-2, to protect cells from excessive Na^+ loading and hyperosmotic stress and to protect the animal from hypertension.

ENaC | hyperosmolarity | sodium | Nedd4L | HECT

Significance

E3 ubiquitin ligases play critical roles in controlling most cellular processes; hence deciphering how their catalytic activity is regulated is essential. This is critical for E3 Nedd4-2, which suppresses the epithelial sodium channel ENaC by targeting it for ubiquitination and degradation; mutations in ENaC that impair binding to Nedd4-2 cause Liddle syndrome, a hereditary hypertension caused by excess ENaC. We found that increased intracellular sodium and osmolarity by ENaC (or other means) lead to stimulation of catalytic activity of Nedd4-2. This work shows that E3 activity can be regulated by ions and by osmolarity, and that ENaC activation leads to stimulation of its own suppressor, Nedd4-2, to prevent excess sodium/fluid loading of cells and hypertension.

Neuronal precursor cell protein expressed developmentally down-regulated 2 (Nedd4-2, or Nedd4-like [Nedd4L]) is an E3 ubiquitin ligase consisting of a C2-WW(x4)-HECT domain architecture; the C2 domain regulates calcium-dependent membrane association; the WW domains recognize and bind substrates, usually those containing PY motifs (L/PPxY); and the HECT domain mediates catalytic activity (1–9).

Tight regulation of catalytic activity of E3 ligases is essential to prevent nonspecific, widespread ubiquitination and degradation of cellular proteins. While studies in recent years have begun to analyze how catalytic activity of some E3s is regulated, including the regulation of Nedd4-1 by Tyr phosphorylation (10), calcium (11), and ubiquitin-mediated trimerization of an α-helix in the HECT domain (12), how catalytic activity of Nedd4-2 is regulated is less clear. This deficiency is significant, given the important role Nedd4-2 plays in regulating ion channels and transporters in several epithelial tissues critical for body homeostasis and animal physiology, primarily the epithelial Na^+ channel ENaC (*SCNN*, see below), but also cotransporters such as NCC (*SLC12A3*) (13) and NKCC1 (*SLC12A1/2*) (14).

One of the best-characterized substrates of Nedd4-2 is ENaC (15, 16), a channel located at the apical membrane (lumen) of salt- and fluid-transporting epithelia, such as those in the distal nephron, lung, and the distal colon (17, 18). ENaC regulates salt and fluid absorption in these (and other) tissues and controls blood pressure (17), lung fluid clearance (19), colonic fluid absorption (20), and other functions. ENaC comprises three subunits: αβγENaC (16, 21, 22), with each subunit containing two transmembrane (TM) domains, a large extracellular domain that in α- and γENaC includes protease cleavage sites (23), and cytosolic N and C termini. The C terminus of each subunit contains a PY motif (1, 24) that binds Nedd4-2 (5, 7); mutations in these PY motifs, which impair Nedd4-2 binding, cause Liddle syndrome, a hereditary hypertension (25, 26). The N termini of α- and γENaC contain Lys residues that serve as ubiquitination sites by Nedd4-2 (27). Ubiquitinated ENaC is targeted for endocytosis and sorting to the lysosome for degradation (8, 28). This contributes to the regulation of salt/fluid homeostasis in the body, by reducing abundance of ENaC at the cell surface and thus diminishing Na^+ influx into cells and Na^+ and fluid reabsorption into the blood stream.

As indicated above, ENaC is activated by cleavage of its ectodomains by proteases (29), releasing inhibitory fragments from the extracellular domains of α- or γ- (but not β)-ENaC (30–36). αENaC is cleaved by the Golgi-resident protease Furin at two sites,

Author affiliations: [a]Cell Biology Program, The Hospital for Sick Children, University of Toronto, Toronto, ON, Canada M5G 0A4; and [b]Department of Biochemistry, University of Toronto, Toronto, ON, Canada M5G 0A4

Author contributions: A.P. and D.R. designed research; A.P., C.J., Z.L., and G.K. performed research; A.P. and W.L.D. contributed new reagents/analytic tools; A.P., C.J., and G.K. analyzed data; and A.P. and D.R. wrote the paper.

The authors declare no competing interest.

This article is a PNAS Direct Submission.

[1]To whom correspondence may be addressed. Email: drotin@sickkids.ca.

This article contains supporting information online at http://www.pnas.org/lookup/suppl/doi:10.1073/pnas.2122495119/-/DCSupplemental.

Published July 18, 2022.

releasing an inhibitory fragment that contain a key 8-residue tract, which leads to partial activation of the channel by increasing channel open probability (Po). Further cleavage of γENaC by Furin at the Golgi and a second extracellular protease lead to the release of a >40-residue inhibitory fragment. Releasing both inhibitory tracts from α- and γENaC results in strong channel activation (reviewed in ref. 29). The protease cleavage sites in α- or γENaC are located in their extracellular GRIP domain (21, 22), and such cleavage is predicted to change ENaC conformation, thus enhancing Na^+ influx through the channel. Interestingly, Nedd4-2 was shown to preferentially induce endocytosis and degradation of proteolytically cleaved (i.e., active) ENaC in cells (37). Accordingly, ubiquitinated cleaved α- and γ- (but not β)-ENaC subunits were identified in rat kidneys, and ubiquitination of a mutant γENaC with impaired binding to Nedd4-2 (a Liddle syndrome mutant) exhibited reduced ubiquitination (38). The mechanism(s) for Nedd4-2–mediated targeting of cleaved, active ENaC for degradation is not known.

Here we show that the catalytic activity of Nedd4-2 is increased by elevated intracellular Na^+ concentration and by increased osmolarity, providing a first demonstration of regulation of catalytic activity of an E3 ubiquitin ligase by ions and osmolarity. We also identify regulatory pathways that mediate this enhanced enzymatic activity of Nedd4-2: p38-MAPK and WNK kinases. Moreover, we decipher how activation of ENaC by proteases (which increases intracellular Na^+ concentration and elevates osmolarity), leads to Nedd4-2–mediated suppression of ENaC (without affecting binding between ENaC and Nedd4-2), thus preventing excessive Na^+ loading of cells by active ENaC, and consequently preventing hypertension.

Results

Cell surface ENaC is down-regulated by Nedd4-2, which binds to and ubiquitinates the channel at the plasma membrane (*SI Appendix*, Fig. S1*A*), leading to its endocytosis and degradation (described above). Previous work has demonstrated that Nedd4-2 preferentially induces endocytosis and degradation of proteolytically cleaved, active ENaC (37). Furin, a serine protease, cleaves α- and γENaC at their extracellular domains as newly formed channels mature through the biosynthetic/Golgi pathway (29) (Fig. 1*A* and *B* and *SI Appendix*, Fig. S1*B*). Activated ENaC then leads to influx of Na^+ into cells, and excessive Na^+ loading results in increased osmolarity. An unsolved question is how Nedd4-2 preferentially targets proteolytically cleaved active ENaC for endocytosis and degradation. Two possibilities can be envisioned: Either a conformational change upon ENaC activation by proteolytic cleavage enables Nedd4-2 binding to the channel, or channel activation and the ensuing Na^+ influx into cells (and elevated osmolarity) promotes Nedd4-2 activation, leading to channel ubiquitination, endocytosis, and degradation. We thus tested both possibilities.

Binding of Nedd4-2 to ENaC Is Independent of Channel Cleavage/Activation by Furin. To determine whether binding of Nedd4-2 to ENaC is dependent upon proteolytic cleavage of the channel, we treated Madin-Darby canine kidney (MDCK) cells stably expressing tagged ENaC [HA(x3)-tagged αENaC, T7 and myc-tagged βENaC, and Flag-tagged γENaC, i.e., $\alpha_{HA;}\beta_{Myc,T7;}\gamma_{Flag}$-ENaC (hereafter called ENaC-MDCK cells] (8) with a Furin inhibitor (FI) and performed coimmunoprecipitation experiments. As seen in Fig. 1*A*, ENaC coimmunoprecipitated endogenous Nedd4-2 to a similar extent in both control cells and cells treated with a FI. Moreover, expression of protease-resistant mutant of ENaC, called Furin mutant (FM), in which the Furin cleavage sites in the α- and γ-subunits are mutated (39, 40) in HEK293T (human kidney) cells together with wild-type (WT) βENaC did not reduce the ability of endogenous Nedd4-2 to bind to this mutant channel relative to the WT channel (Fig. 1*B*). The same results were obtained with a catalytically inactive Nedd4-2(CS) (*SI Appendix*, Fig. S1*C*). These results suggest that the binding of Nedd4-2 to ENaC is independent of proteolytic cleavage and activation of the channel.

Elevated $[Na^+]_i$ by Active ENaC or by Monensin Increases Enzymatic Activity of Nedd4-2. As ENaC activation or inhibition did not affect the ability of Nedd4-2 to bind this channel, we tested whether ENaC activation and the ensuing elevated intracellular Na^+ ($[Na^+]_i$) can affect enzymatic activity of Nedd4-2. First, we tested the effect of elevating ($[Na^+]_i$) with the Na^+ ionophore monensin, which promotes Na^+ influx in exchange for efflux of H^+ (and consequently elevated $[Na^+]_i$ and reduced $[K^+]_i$ levels) (*SI Appendix*, Fig. S2*A*) on (Flag-tagged) Nedd4-2 activity. Following the treatment, lysates from the transfected cells were boiled in sodium dodecyl sulfate (SDS) to remove Nedd4-2–associated proteins, and Nedd4-2 autoubiquitination was determined by immunoprecipitating (IP) with Flag antibodies and immunoblotting with anti-HA (ubiquitin) antibodies. Fig. 1*C–E* shows that treatment of epithelial HEK293T, FRT (Fisher rat thyroid), or MDCK cells with monensin led to increased $[Na^+]_i$, as expected (*SI Appendix*, Fig. S2*A*) and a strong stimulation of enzymatic activity of Nedd4-2, as determined by Nedd4-2 autoubiquitination activity. Nedd4-2 autoubiquitination activity was verified by its loss in cells transfected with the Nedd4-2 catalytically inactive (CS) mutant.

Next, we assessed the effect of ENaC activation and inhibition on catalytic activity of Nedd4-2. As indicated above, proteolytic cleavage of α- or γENaC activates the channel, thus enhancing Na^+ influx through the channel and elevated $[Na^+]_i$ (*SI Appendix*, Fig. S2*B*). We therefore used the above-described proteolytic resistant ENaC mutant expressed in HEK293T cells, along with tagged Nedd4-2 and HA-ubiquitin (HA-Ub), and assessed Nedd4-2 autoubiquitination activity. (We could only use HEK293T cells for these experiments as we could not express five plasmids together in other cell lines to detect sufficient protein expression of each.) Fig. 1*F* shows a significant reduction in enzymatic activity of Nedd4-2 in the Furin resistant mutant (FM) ENaC, in accord with the reduction in ENaC activity and $[Na^+]_i$. This effect was (partially) rescued by treating these mutants with low doses of the more general protease, trypsin, a maneuver known to activate ENaC (41). In agreement with these results, inhibition of ENaC with amiloride also inhibited Nedd4-2 catalytic activity (*SI Appendix*, Fig. S1*D*).

Taken together, these results suggest that enhanced influx of Na^+ into cells via activated ENaC, or by the ionophore monensin, leads to the stimulation of enzymatic activity of Nedd4-2, the suppressor of ENaC.

Elevated Osmolarity and Tonicity Increase Catalytic Activity of Nedd4-2. Enhanced Na^+ influx through active ENaC channels (*SI Appendix*, Fig. S2*B*) increases cellular Na^+ loading (24) and osmolarity, as evidenced by cell swelling (*SI Appendix*, Fig S3*A*). To determine whether increased osmolarity affects Nedd4-2 activity, HEK293T, FRT, MDCK, or mouse kidney cortical collecting duct (CCD) cells (kindly provided by H. Hummler, University of Lausanne, Lausanne, Switzerland) were transfected with either Flag-tagged Nedd4-2 WT or its catalytically inactive mutant [Nedd4-2(CS)] together with HA-Ub, and treated with either

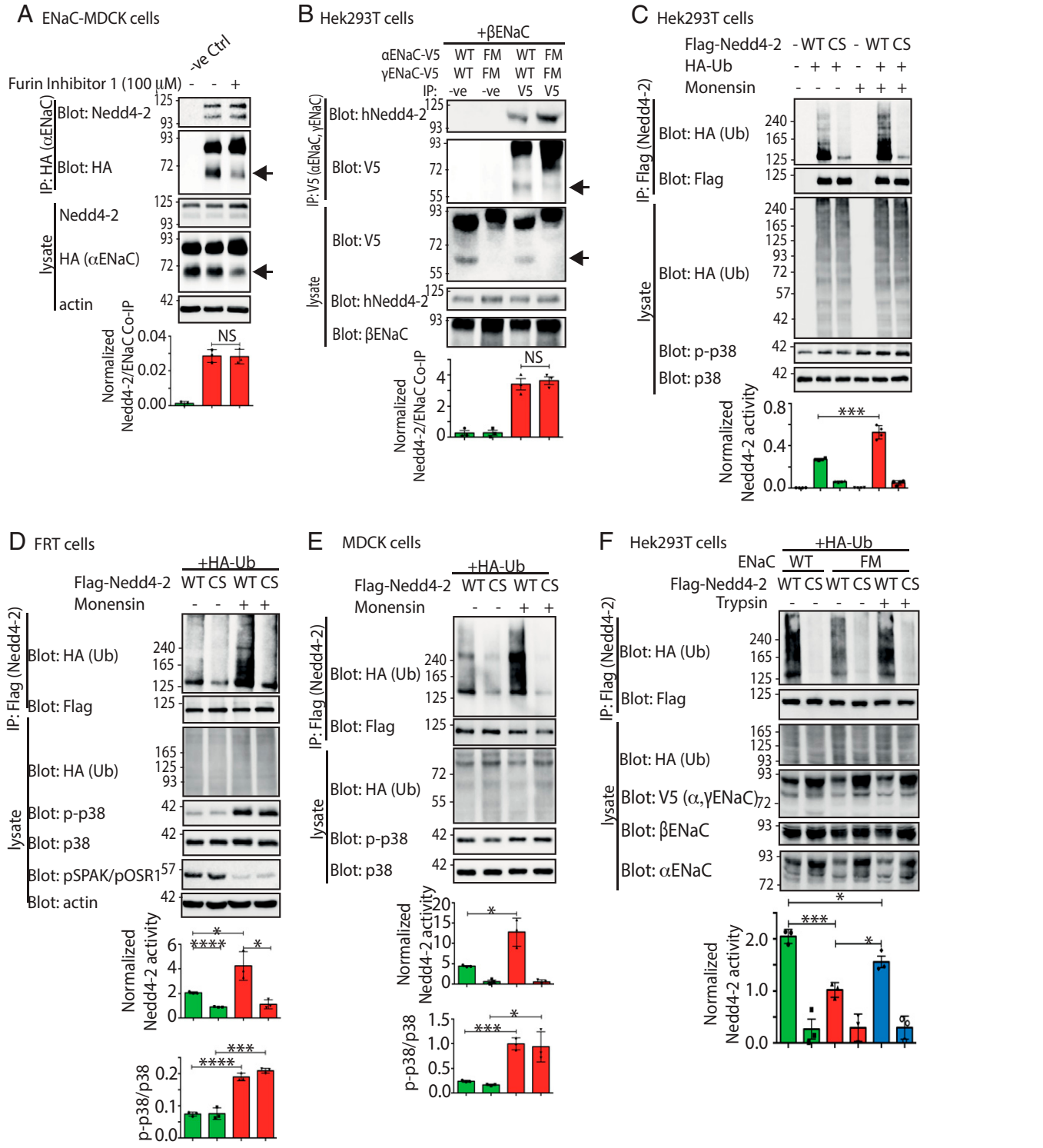

Fig. 1. Na^+ influx via ENaC or monensin enhances Nedd4-2 catalytic activity without affecting Nedd4-2 binding to ENaC. ENaC activity does not affect Nedd4-2:ENaC interactions. (*A*) ENaC-MDCK cells stably expressing tagged ENaC [HA(×3)-tagged αENaC; T7 and myc-tagged βENaC; Flag-tagged γENaC ($\alpha_{HA}\beta_{Myc,T7}\gamma_{Flag}$-ENaC)], were treated (or not) with 100 μM Furin inhibitor 1 for 2 d to inhibit ENaC activity. Following HA IP, the presence of coimmunoprecipitated Nedd4-2 was verified by immunoblotting with Nedd4-2 antibodies. Negative control (-ve Ctrl): IP from ENaC-MDCK cell lysate using Protein G beads and mouse IgG. (*B*) HEK293T cells were transfected with either WT ENaC (V5-tagged αENaC, untagged βENaC, and V5-tagged γENaC [$\alpha_{V5}\beta\gamma_{V5}$-ENaC]) or FM ENaC (V5-tagged αR205A/R208A/R231A ENaC, untagged βENaC, and V5-tagged γR143A ENaC [$\alpha_{R205A/R208A/R231A\text{-}V5}\beta\gamma_{R143A\text{-}V5}$-ENaC]), and the presence of coimmunoprecipitated Nedd4-2 was determined by IP with V5 antibodies and immunoblotting for Nedd4-2. Arrows represent cleaved ENaC subunits. Increased $[Na^+]_i$ by the ionophore monensin elevates Nedd4-2 activity. (*C*–*E*) HEK293T (*C*), FRT (*D*), or MDCK (*E*) cells were transfected with either Flag-tagged WT Nedd4-2 or its catalytically inactive (CS) mutant, plus HA-tagged ubiquitin (HA-Ub), and treated with 40 μM monensin for 30 min where indicated. Nedd4-2 catalytic activity was assessed by boiling lysates in SDS, IP of Nedd4-2 using FLAG-agarose beads, and immunoblotting with anti-HA antibodies. Active ENaC enhances Nedd4-2 catalytic activity in cells. (*F*) HEK293T cells were transfected with HA-tagged Ub and either WT ENaC ($\alpha_{V5}\beta\gamma_{V5}$-ENaC), FM ENaC ($\alpha_{R205A/R208A/R231A\text{-}V5}\beta\gamma_{R143A\text{-}V5}$-ENaC) and Flag-tagged Nedd4-2 WT or CS mutant, as indicated. Where indicated, cells were treated with 10 μg/mL trypsin type 1 for 1 h prior to lysis. Nedd4-2 catalytic activity was determined as described above. (*C*–*F*) Quantification of Nedd4-2 catalytic activity and p38 activation (phosphorylation) is depicted below their respective blots (mean ± SEM, $n = 3$ independent experiments; *P* values *<0.05; ***<0.001; ****<0.0001; Student's *t* test; NS: not significant). Numbers at the *y* axes of each immunoblot (in all figures) marks molecular weight standards (in kilodaltons).

iso-osmotic (135 mM, 310 mOsm) or hyperosmotic (270 mM, 580 mOsm) NaCl solution. Such increased osmolarity led to elevated $[Na^+]_i$, with minimal or no effect on $[K^+]_i$ (*SI Appendix*, Fig. S2*C*). As shown in Fig. 2*A*–*D*, our results reveal a significant increase in Nedd4-2 catalytic activity (autoubiquitination) in HEK293T, FRT, MDCK, and CCD cells treated with hyperosmotic NaCl solution relative to the isoosmotic NaCl control. Elevated Nedd4-2 enzymatic activity was already detected upon incubation of cells in the presence of 400 mOsm (180 mM) NaCl and further increased with escalating osmolarity, as exemplified in CCD and HEK293T cells (Fig. 2*D* and *SI Appendix*, Fig. S3*B*). Of note, Nedd4-2 localization in FRT cells under normal, isoosmotic conditions was confined to the cytoplasm and the plasma membrane regions, and increased cellular osmolarity did not alter this distribution (*SI Appendix*, Fig. S3*C*).

To investigate this effect in a tissue model, we tested the effect of hyperosmolarity on Nedd4-2 activity in organoids derived from mouse distal colon, which we and others previously showed robustly express Nedd4-2 and ENaC (14–16, 20). For this, organoids were extracted from the Matrigel and treated with hyperosmotic (270 mM) NaCl or isoosmotic (135 mM) NaCl control solutions. Lysates were incubated with tandem ubiquitin binding entities (TUBEs) agarose to capture ubiquitinated proteins and endogenous ubiquitinated Nedd4-2 then detected by immunoblotting with Nedd4-2 antibodies. As shown in Fig. 2*E*, there was a significant increase in the amount of ubiquitinated Nedd4-2 (relative to total precipitated ubiquitin) in organoids treated with hyperosmotic solution vs. isoosmotic control solution, although we cannot preclude the possibility of other ubiquitinated proteins coprecipitating with Nedd4-2.

To test whether NaCl can directly activate Nedd4-2, we assayed the catalytic activity of purified Nedd4-2 in vitro when treated with increasing concentrations of NaCl. Our results show that Nedd4-2 activity was actually inhibited with increasing NaCl concentrations (*SI Appendix*, Fig. S1*E*), possibly by affecting protein conformation at high salt concentrations.

To decipher the ionic requirement for promoting increased Nedd4-2 activity in cells placed under hyperosmotic conditions, Nedd4-2 activity assays were conducted as described above in HEK293T cells, except cells were treated with hyperosmotic or isoosmotic control solutions composed of either NaCl, NMDG-Cl^- (depletes Na^+ from cells), or Na^+-gluconate (depletes Cl^- from cells), each at 270 mM (compared to 135 mM in the isoosmotic controls) (*SI Appendix*, Fig. S2*C*). Our results show that all these hyperosmotic solutions were able to increase Nedd4-2 catalytic activity (*SI Appendix*, Fig. S3*E*). Moreover, elevated tonicity achieved by incubating cells with sorbitol also increased Nedd4-2 catalytic activity (*SI Appendix*, Fig. S3*E*). Sorbitol does not permeate cells, nor did it affect $[Na^+]_i$ or $[K^+]_i$ in the time frame of the experiment (*SI Appendix*, Fig. S2*C*) (although over time it could affect cellular ion transport due to changes in ionic strength and cell shrinkage). Thus, hyperosmolarity and hypertonicity per se can enhance enzymatic activity of Nedd4-2.

Collectively, these results suggest that increased $[Na^+]_i$ (by active ENaC or by monensin) and increased osmolarity or tonicity in cells increases Nedd4-2 catalytic activity, and this is not due to a direct effect of ions (such as Na^+ or Cl^-) on Nedd4-2. We thus searched for the signaling events that mediate the activation of enzymatic activity of Nedd4-2, focusing on p38-MAPK (p38) and WNK kinases, two known sensors of osmolarity.

Activated p38 and WNK Inhibition Both Enhance the Catalytic Activity of Nedd4-2 under Hyperosmotic Stress. Hyperosmotic stress has been shown to activate p38 (42, 43), as also observed in our studies in four different cell lines (HEK293T, FRT, MDCK, and CCD) (Fig. 2*A*–*D* and *SI Appendix*, Fig. S3*D* and *E*), as well as in colonic organoids treated in situ in the Matrigel in which they are grown (Fig. 2*E*). We also found that monensin treatment enhanced p38 activation (p-p38) (Fig. 1*D* and *E*). Since increased Nedd4-2 activity is correlated with increased p-p38 under hyperosmotic stress, we interrogated whether p-p38 is involved in mediating the activation of Nedd4-2 by elevated osmolarity. Thus, we tested the effect of the p38 inhibitor, BIRB796, on Nedd4-2 activity. Our results show that BIRB796 abolished the hyperosmotic NaCl (Fig. 3*A*) or monensin (*SI Appendix*, Fig. S4*A*)-stimulated increase of catalytic activity of Nedd4-2 in HEK293T cells, and CCD cells (Fig. 3*B*). [Note that BIRB796 does not inhibit p38 signaling in MDCK cells (*SI Appendix*, Fig. S5*A*), hence was not studied further in these cells]. These data suggest that p38 activation stimulates the catalytic activity of Nedd4-2 under hyperosmotic conditions and under elevated $[Na^+]_i$ (Fig. 3*E*).

Hyperosmotic stress is also known to activate the WNK kinases and their downstream kinase substrates, SPAK and OSR1 (44) (see also Fig. 3*A*–*C*). We therefore investigated whether WNK/SPAK/OSR1 also regulates Nedd4-2 catalytic activity under hyperosmotic conditions by using WNK1-knockout HEK293T cells (WNK1-KO) (45). Surprisingly, Nedd4-2 activity was significantly enhanced in WNK1-KO cells compared to control cells under both isoosmotic and hyperosmotic NaCl (Fig. 3*C*) or after monensin treatments (*SI Appendix*, Fig. S4*B*). This effect was even further enhanced when cells (control and WNK1-KO) were treated with the pan-WNK-kinase inhibitor, WNK463, that inhibits WNK1-4 (Fig. 3*C* and *D*), an effect also observed in ENaC-MDCK cells treated with 1 to 10 μM of WNK463 (Fig. 3*D* and *SI Appendix*, Fig. S4*C*). This suggests that multiple WNK family members may contribute to the suppression of Nedd4-2 activity. Of note, endocytosis of the cleaved, active form of ENaC (shown here for αENaC) was more sensitive to low doses of WNK463 than the uncleaved form of the channel (*SI Appendix*, Fig. S4*C*, *Bottom*). As well, we noticed an increase in active p-MK2, the downstream target of p-p38, in the WNK1-KO cells under both isoosmotic and hyperosmotic NaCl conditions (Fig. 3*C*), as we also found in WT cells treated with WNK463. While this suggests that WNKs can (partially) suppress p38 signaling, this inhibition only accounts for a fraction of WNK-mediated suppression of Nedd4-2 activity (*SI Appendix*, Fig. S5*B*). Interestingly, while hyperosmotic NaCl treatment activated WNK signaling, treatment of cells with monensin suppressed WNK signaling (Fig. 1*D* and *SI Appendix*, Figs. S4*B* and S6). Although hyperosmotic NaCl activated WNK signaling, the p38 activation under these conditions caused Nedd4-2 to be hyperactivated, and Nedd4-2 activity was further increased when WNK inhibitors were added (Fig. 3*C*).

Taken together, these data suggest that the WNK kinases (especially WNK1), which are activated by hyperosmolarity, act as suppressors of enzymatic activity of Nedd4-2, while p38 stimulates Nedd4-2 activity under these conditions (Fig. 3*E*).

Active ENaC Increases $[Na^+]_i$, Suppresses WNK Signaling, and Promotes p38 Activation. Active ENaC is known to promote entry of sodium into cells and to elevate $[Na^+]_i$ (see also *SI Appendix*, Fig. S2*B*), which then increases osmolarity (*SI Appendix*, Fig. S3*A*). We thus investigated whether this increase in $[Na^+]_i$ affects p38 and WNK signaling. To address this, we induced the expression of tagged ENaC stably expressed in a MDCK cell line [called ENaC-MDCK) (8), a kidney cell line that forms a polarized epithelial monolayer with active ENaC]. We first measured $[Na^+]_i$ without or with amiloride treatment, which blocks ENaC

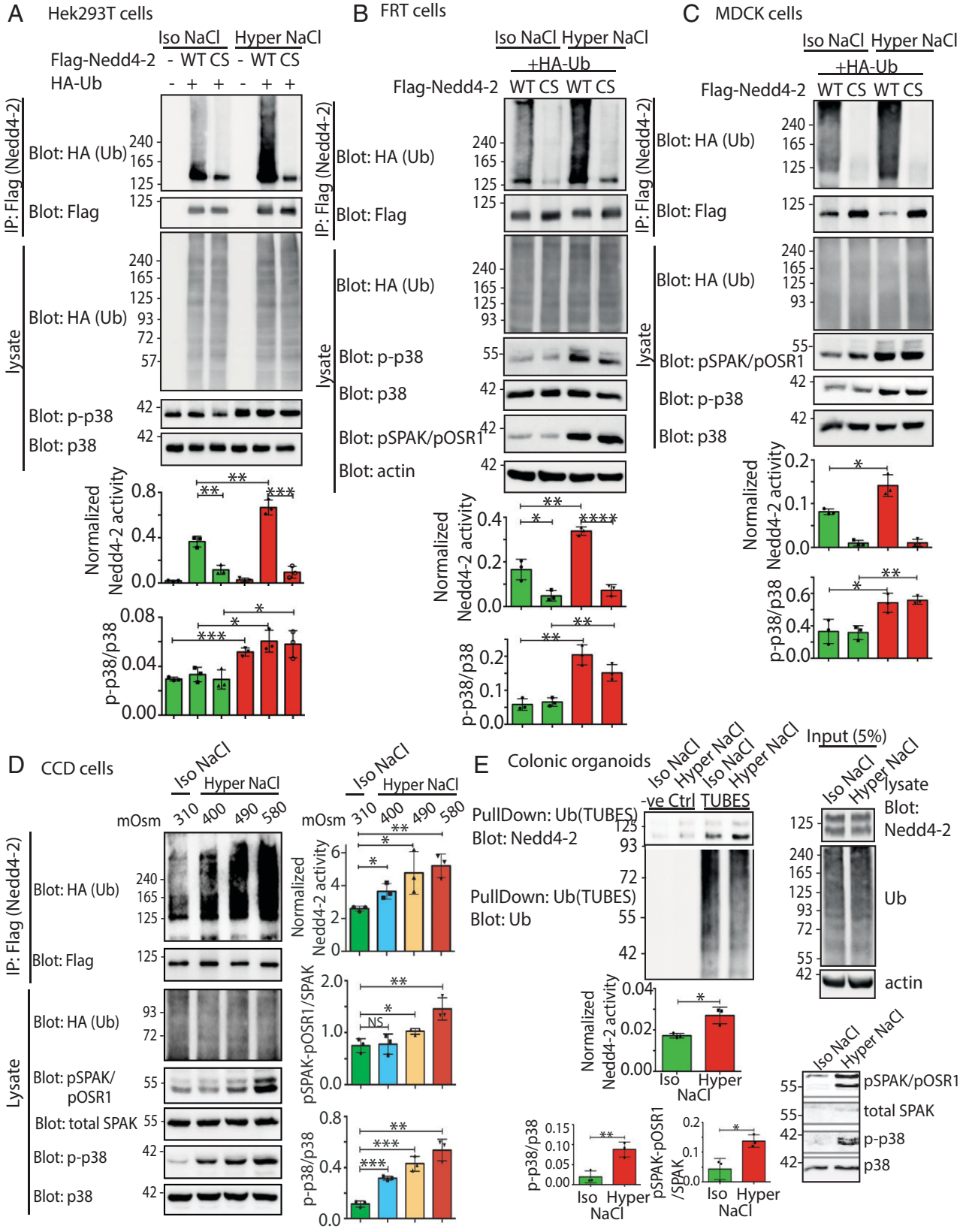

Fig. 2. Elevated osmolarity enhances Nedd4-2 catalytic activity in cells and mouse colonic organoids. (*A–D*) HEK293T (*A*), FRT (*B*), MDCK (*C*), or mouse CCD (*D*) cells were transfected with either Flag-tagged Nedd4-2 WT or Nedd4-2 (CS) and HA-Ub, and treated with either isoosmotic (iso, 135 mM, 310 mOsm) or hyperosmotic (hyper, 270 mM, 580 mOsm) NaCl solution, or escalating concentrations of NaCl in *D*, for 15 min. Nedd4-2 catalytic activity was determined as described in Fig. 1 and *Lower* panels represent controls. (*E*) Mouse colonic organoids were treated with either isoosmotic or hyperosmotic (580 mOsm) NaCl solution for 15 min prior to lysis and Nedd4-2 catalytic activity was assessed by IP of ubiquitin using TUBEs agarose and immunoblotting for Nedd4-2. Quantification of Nedd4-2 catalytic activity and WNK and p38 activation (SPAK/OSR1 and p38 phosphorylation, respectively) is depicted below their respective blots, where indicated (mean ± SEM, $n = 3$ independent experiments; P values *<0.05; **<0.01; ***<0.001; ****<0.0001 Student's t test; NS: not significant).

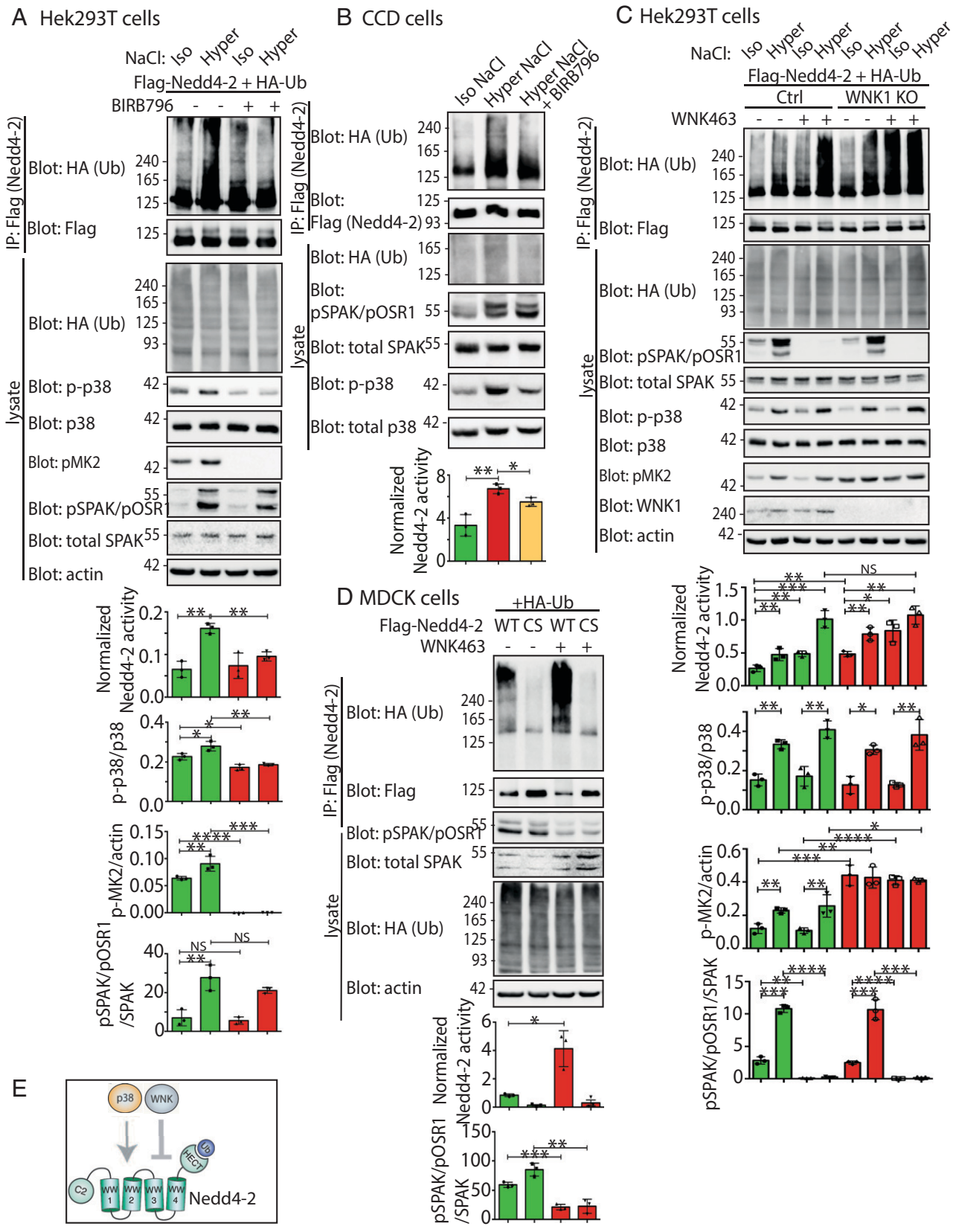

Fig. 3. p38 activation and WNK inhibition enhance Nedd4-2 catalytic activity. HEK293T cells (*A* and *C*), CCD cells (*B*), or uninduced ENaC-MDCK cells (*D*) (behaving as untransfected MDCK cells) were transfected with either Flag-tagged Nedd4-2 WT or its Nedd4-2 (CS) mutant, where indicated, plus HA-Ub, and then treated with either (*A* and *B*) 2 μM BIRB796 (p38 inhibitor), or (*C* and *D*) 10 μM WNK463 (pan-WNK inhibitor), for 2 h followed by incubation in either hyperosmotic NaCl (hyper, 580 mOsm) or iso-osmotic (iso 310 mOsm) control solutions for 15 min in the absence/presence of the p38 or WNK inhibitor. Nedd4-2 catalytic activity was determined as described in Fig. 1. Quantification of Nedd4-2 catalytic activity, as well as WNK (pSPAK/pOSR1) and p38 (p-p38) activation (phosphorylation) is depicted below their respective blots (mean ± SEM, $n = 3$ independent experiments; P values *<0.05; **<0.01; ***<0.001; ****<0.0001 Student's t test. NS: not significant). (*E*) Model of regulation of Nedd4-2 catalytic activity in cells by WNK and p38.

channel activity. As expected, inducing ENaC expression in the ENaC-MDCK cells resulted in an increase in $[Na^+]_i$ (and a corresponding decrease in $[K^+]_i$) (*SI Appendix*, Fig. S2*B*), and this was significantly reduced upon treatment with amiloride. Elevated ENaC expression, causing elevated $[Na^+]_i$, led to both p38 activation and WNK suppression (reduced p-SPAK/p-OSR1 phosphorylation) (Fig. 4*A*); this effect was similar to that of monensin in HEK293T cells (Fig. 1*D* and *SI Appendix*, Figs. S4*B* and S6) and was attenuated upon treatment with the ENaC inhibitors amiloride or benzamil, or by blocking ENaC cleavage/activation with a Furin inhibitor (Fig. 4*A* and *B*). Thus, active ENaC and elevated $[Na^+]_i$ enhance p38 activity and suppress WNK signaling.

Interestingly, treatment of cells with amiloride, which blocked ENaC channel activity and reduced intracellular Na^+ concentration in MDCK cells (*SI Appendix*, Fig. S2*B*), resulted in stabilization of the cleaved (active) αENaC and γENaC (but not βENaC, which is not cleaved by proteases) (Fig. 4*A* and *B*). These results suggest that in the presence of amiloride, ENaC channel activity is inhibited and this reduces intracellular Na^+ concentration, promoting WNK signaling and reducing p38 activation; the combined effect on these signaling pathways reduces Nedd4-2 catalytic activity in cells, as indeed we observed here (*SI Appendix*, Fig. S1*D*). As a result, more ENaC is present on the cell surface (Fig. 4*C*).

Since our results above show that WNK inhibition promotes Nedd4-2 activity, we predicted that this Nedd4-2 stimulatory maneuver would suppress ENaC. Indeed, we found that the WNK inhibitor WNK463 increased ubiquitination of cell surface ENaC and, accordingly, severely reduced the amount of ENaC at the cell surface in both ENaC-MDCK (Fig. 4*C*) and HEK293T cells that ectopically expressed ENaC (*SI Appendix*, Fig. S7*A* and *B*). In agreement, ENaC activity was strongly inhibited by WNK463 in ENaC-MDCK cells (Fig. 4*D*), and accordingly, endocytosis of the cleaved, active αENaC exhibited much greater sensitivity to escalating doses of WNK463 than the uncleaved form of αENaC (*SI Appendix*, Fig. S4*C*). The reduction of cell surface ENaC by the WNK inhibitor is mediated by Nedd4-2, because a catalytically inactive Nedd4-2(CS) mutant restores the elevated ENaC levels in cells treated with this same WNK inhibitor (*SI Appendix*, Fig. S7*A*). These results suggest that the suppressive effects of WNKs on Nedd4-2 activity, in turn, affect ENaC cell surface levels (especially cleaved, active ENaC), and function (Fig. 4*E*).

As indicated above, BIRB796 does not block p38 activation in MDCK cells, and accordingly, had no effect on cell surface stability of ENaC, nor did it affect ENaC function/activity in these cells. In HEK293T cells, BIRB796 has a small/variable inhibitory effect on p-p38 (and a significant inhibitory effect on pMK2, the downstream effector of p38) (*SI Appendix*, Fig. S6), which translated into a small, albeit significant, suppressive effect on Nedd4-2 activity (*SI Appendix*, Fig. S4*A*). Yet, this small suppressive effect was not strong enough to alter ubiquitination or stability of cell surface ENaC (*SI Appendix*, Fig. S7*A* and *B*). This suggests that the effect of WNK (which partially inhibits p38) (*SI Appendix*, Fig. S5*B*) is more dominant than that of p38 with regards to the regulation of ENaC stability.

Discussion

Our studies here show that elevated intracellular Na^+ brought about by either activation of ENaC or by use of the Na^+ ionophore monensin, and increased osmolarity or tonicity, lead to stimulation of catalytic activity of Nedd4-2; this likely occurs via activation of p38 and/or suppression of WNK kinases (Fig. 4*E*). It, in turn, leads to the suppression of ENaC by the activated Nedd4-2 to prevent Na^+ loading of cells.

To our knowledge, this work represents the first demonstration of regulation of catalytic activity of an E3 ligase by elevated intracellular Na^+ and elevated osmolarity or tonicity. While the results shown here focus on Nedd4-2, which is known to suppress several epithelial ion channels and transporters (e.g., ENaC, NCC, and NKCC1) (5, 7, 8, 13, 14) it is likely that this type of enzymatic regulation extends to other E3 ligases, which remains to be investigated.

Although we demonstrate that elevated intracellular $[Na^+]$ and osmolarity lead to stimulation of enzymatic activity of Nedd4-2, this effect is indirect and involves at least two stress-response pathways: p38-MAPK, which stimulates Nedd4-2 catalytic activity, and WNK, which inhibits it (Fig. 4*E*). These two pathways are known to be activated by hyperosmolarity (44, 46, 47). How exactly do p38 and WNK regulate catalytic activity of Nedd4-2 is not known currently. Notably, Nedd4-2 is well documented to be phosphorylation (on S448 and S532, human Nedd4-2) by SGK1 and Akt (48, 49) and other kinases, providing binding sites for 14-3-3 proteins, which then interfere with the ability of Nedd4-2 to bind and suppress ENaC (50). While we observed that inhibiting SGK1 or PKA did not affect Nedd4-2 activity, we nevertheless found a reduction in Nedd4-2 phosphorylation on S448 and S532 under hyperosmotic conditions (*SI Appendix*, Fig. S8). This is consistent with a better ability of hypophosphorylated Nedd4-2 to bind to and suppress ENaC. Thus, our data do not support the notion that such hypophosphorylation affects Nedd4-2 catalytic activity (*SI Appendix*, Fig. S8), suggesting that the p38-mediated stimulation of Nedd4-2 activity is not mediated via SGK1 or PKA.

In accordance with our observed stimulatory effect of p38 and inhibitory effect of WNKs on catalytic activity of Nedd4-2, cell surface ENaC was reduced after treatment with WNK inhibitors (due to Nedd4-2 stimulation), but inhibition of p38 had little effect on ENaC stability at the cell surface. Although, as indicated above, it is not yet known how exactly p38 and WNK regulate catalytic activity of Nedd4-2, some of our results suggest that WNK itself can suppress p38 function, which could partially (but not completely) explain WNKs' ability to inhibit Nedd4-2 activity. Curiously, earlier work had demonstrated that the accumulation of intracellular Na^+ causes ENaC self (auto)-inhibition, but suggested that while Na^+ itself is the trigger for such an effect, Na^+ per se does not cause it directly; rather, such self (auto)-inhibition is caused by other mediators that were not identified at the time (51). Our work here suggests that p38-MAPK, WNKs, and Nedd4-2 may be such mediators, or at least contributors, to the regulation of self (auto)-inhibition of ENaC. Currently, we cannot preclude the possibility that other factors, such as deubiquitinating enzymes (DUBs), previously shown to regulate ENaC ubiquitination status and degradation (52–54), also participate in regulating the osmotic-mediated activation of Nedd4-2, and hence suppression of ENaC.

In agreement with our findings here, Staub and Gamba and coworkers (55) showed earlier that WNK3 can prevent Nedd4-2 from suppressing its substrate NCC (a kidney Na^+/Cl^- transporter), and suggested that WNK3 may attenuate Nedd4-2 function, although they did not elucidate how this may take place. In addition, work from the Lifton and coworkers showed that the RING E3 ligase KLHL3-Cul3 binds to and degrades WNK4 (56), the enhancer of NCC and suppressor of the K^+ channel ROMK; mutations in WNK4 or KLHL3 that prevent binding to each other stabilize WNK4, resulting in enhanced expression/function of NCC and reduced levels of ROMK in the kidney;

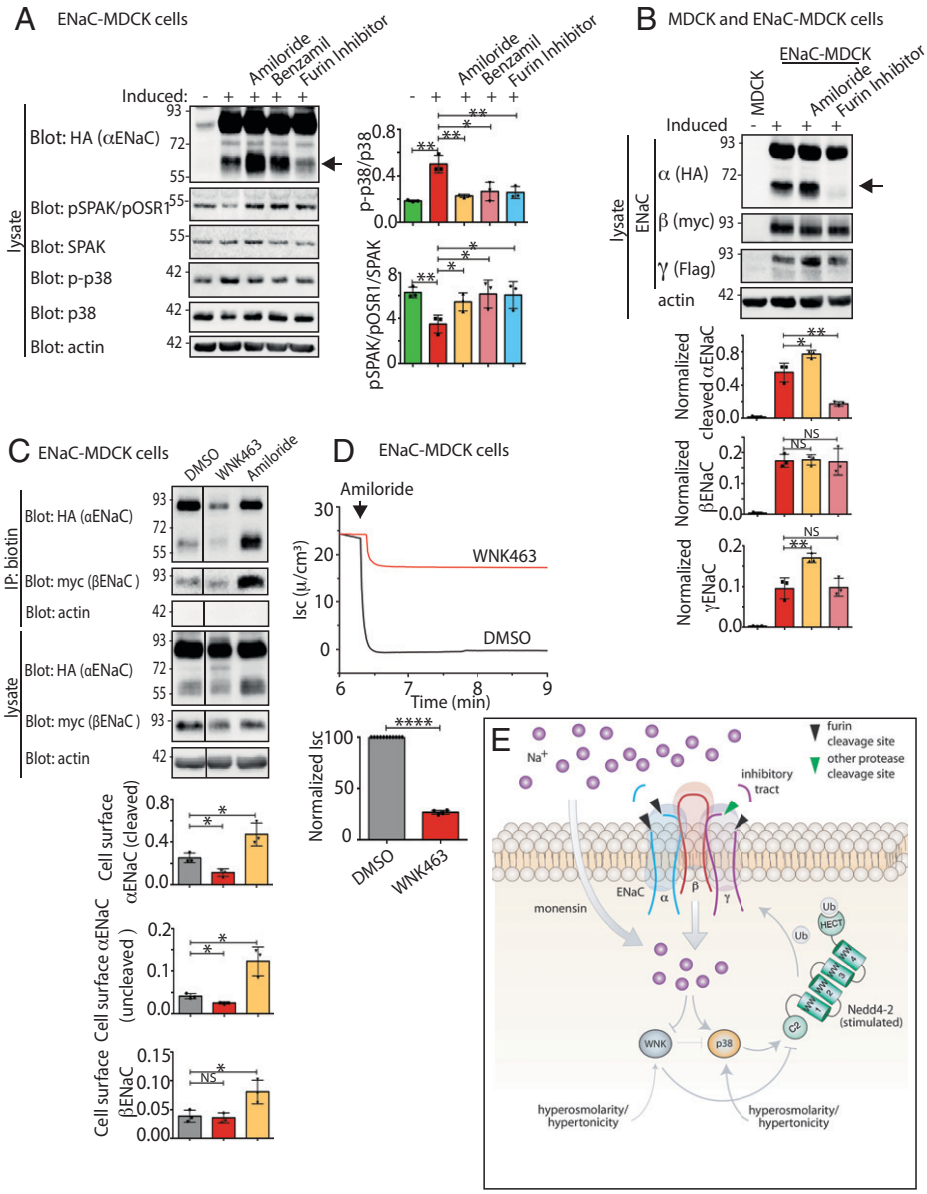

Fig. 4. Active ENaC suppresses WNK signaling and promotes p38 activation in MDCK cells. (*A* and *B*) ENaC-MDCK cells stably expressing tagged ENaC ($\alpha_{HA}\beta_{Myc,T7}\gamma_{Flag}$-ENaC) were treated with 10 μM amiloride (ENaC inhibitor), 1 μM benzamil (a high specificity ENaC inhibitor), or 100 μM Furin inhibitor 1 for 2 d, and levels of α-, β-, and γENaC subunits, activated p38 (p-p38), or activated WNK substrates (pSPAK/pOSR1) analyzed. In *A*, the ENaC-MDCK cells were induced (or not) to express the tagged ENaC, as indicated (*Materials and Methods*). (*C*) WNK inhibition destabilizes cell surface ENaC and reduces its activity: ENaC-MDCK cells were treated with either 10 μM WNK463 (2 h) or 10 μM amiloride (2 d) before biotinylating the cell surface proteins. Following streptavidin IP, the stability of ENaC subunits was assessed by immunoblotting with HA (αENaC) or myc (βENaC) antibodies. (*D*) ENaC function (Isc) analyzed in Ussing chambers in the ENaC-MDCK cells following treatment (or not) with 10 μM WNK463 for 2 h. Traces are from one representative experiment (arrow: apical addition of the ENaC inhibitor amiloride, 10 μM). Quantitation of 4 to 10 independent experiments (mean ± SEM) of amiloride-sensitive Isc (ENaC) in the absence/presence of WNK463 is presented below the traces. *P* values *<0.05; **<0.01; Student's *t* test; NS: not significant). (*E*) Summary model of regulation of Nedd4-2 catalytic activity in cells by sodium influx via ENaC or monensin, as well as by hyperosmolarity/hypertonicity, and the consequence for ENaC ubiquitination by Nedd4-2, and hence for cell surface stability of this channel.

this leads to increased Na^+ and fluid reabsorption (causing hypertension) and decreased K^+ excretion (causing hyperkalemia). Accordingly, inactivating mutations in KLHL3 or Cul3 (which stabilize WNKs) cause PHAII (pseudohypoaldosteronism type II), a disease characterized by hyperkalemia and hypertension (57).

One of the best-known in vitro and in vivo substrates for Nedd4-2 is ENaC (2, 5, 8, 14, 38, 58, 59), which when activated leads to influx of Na^+, elevated $[Na^+]_i$, and osmolarity. Therefore, we hypothesized that activation of ENaC, commonly mediated by Furin and other proteases (23), should enhance Nedd4-2 enzymatic activity. Indeed, our results show that ENaC bearing mutations at its Furin cleavage sites, which exhibit reduced channel activity and reduced $[Na^+]_i$, lead to a reduction in Nedd4-2 enzymatic activity; this reduction can be rescued with an alternative protease, trypsin (41), which partially restores $[Na^+]_i$ levels and Nedd4-2 catalytic activity in the ENaC Furin mutants. It is therefore the enhanced Nedd4-2 catalytic activity, and not the ability of Nedd4-2 to bind ENaC (since Nedd4-2 can bind both cleaved/active and uncleaved channels), which controls the regulation of ENaC by Nedd4-2. These results help provide an explanation for the observation that Nedd4-2 preferentially targets the cleaved, active ENaC for degradation (37, 38), since more active ENaC and elevated Na^+ influx stimulates catalytic activity of Nedd4-2.

An important implication for the present study is that ENaC activation, with the consequent accumulation of intracellular Na^+, leads to activation of its own suppressor, Nedd4-2 (Fig. 4*E*); this ensures that active ENaC is ubiquitinated, endocytosed, and degraded, in order to terminate Na^+ influx into cells and excessive Na^+ loading. Such excessive Na^+ loading can lead to hypertension, as exemplified by Liddle syndrome (26), a hereditary hypertension in which ENaC accumulates at the plasma membrane due to mutations in one of its PY motifs that impairs binding to and suppression by Nedd4-2 (2). An additional negative feedback loop mechanism to regulate active ENaC was proposed by Myerburg and coworkers, who showed that the accumulated intracellular Na^+ following ENaC activation leads to inhibition of subsequent ENaC processing by proteases (60). Both our studies and those of Myerburg and coworkers may help provide explanations for the long-standing observation of feedback inhibition (autoinhibition) of ENaC by elevated intracellular Na^+.

The stimulation of catalytic activity of the ENaC suppressor Nedd4-2 by activated ENaC and elevated $[Na^+]_i$ and osmolarity, provides a mechanism by which E3 ligases are regulated. Such tight regulation is required to ensure E3 ligases are only active at the right time, by the correct upstream effector and toward the correct substrate. Accordingly, we had previously demonstrated activation of catalytic activity of Nedd4-1 by its bona fide substrate, the receptor Tyr kinase (RTK) FGFR1, by disrupting an inhibitory HECT:C2 domain interaction triggered by Tyr phosphorylation within these domains (10). Likewise, the Nedd4 family member Smurf2, known to target TGFβ for degradation, is activated by disrupting its inhibitory C2:HECT interaction by the inhibitory Smad, Smad7, downstream of the activated TGFβ receptor (61). Thus, activation of such transporters and receptors leads to the subsequent activation of their own ubiquitin ligase suppressors, to ensure termination of signaling or excess ion loading within cells.

In sum, our study here identified a mode of regulation of catalytic activity of an E3 ligase, with important implications for the regulation of ENaC and Na^+ and osmotic handling by the cell and the organism.

Materials and Methods

Reagents and solutions are summarized in *SI Appendix*, Tables 1 and 2.

Binding and Ubiquitination Experiments in Cells and Organoids. Cells were transfected for 48 h with either Flag-tagged Nedd4-2 (WT) or its CS mutant, HA-tagged ubiquitin or V5-tagged ENaC (WT or Furin cleavage mutant) (39, 40), kindly provided by T. Kleyman and O. Kashlan, University of Pittsburgh, Pittsburgh, PA, where indicated. Mouse cortical collecting ducts (clone 1) cells (CCD cells) were kindly provided by E. Hummler, University of Lausanne, Lausanne, Switzerland. CCD and FRT cells were transfected using Lipofectamine 3000 reagent (Invitrogen). Briefly, cells were seeded in 6-cm dishes and transfected with DNA–lipid complexes comprising of 2.5 μg each of Flag-Nedd4-2 and HA-Ub plasmids (in 250 μL OPTIMEM with 10 μL P3000) and 15 μL Lipofectamine 3000 reagent (in 250 μL OPTIMEM). In all ubiquitination experiments, cells were treated with 10 μM MG132 for 2 h followed by treatment with either 40 μM monensin (30 min), isoosmotic (310 mOsm), or hyperosmotic (580 mOsm) solutions (*SI Appendix*, Table 2), or other hyperosmotic NaCl concentrations (400 and 490 mOsm, where indicated), or 0.4 M sorbitol, for 15 min at 37 °C.

For drug inhibition experiments, cells were treated with either 2 μM BIRB796 (2 h), 5 μM SB203580 (2 h), 10 μM WNK463 (2 h), 10 μM EMD638683 (2 h), or 20 μM H-89 (1 h), followed by incubation with either 40 μM monensin (30 min) or hyperosmotic NaCl (or isoosmotic NaCl control) (15 min) in the presence of the indicated drug. ENaC-MDCK cells stably expressing tagged ENaC ($\alpha_{HA}\beta_{Myc,T7}\gamma_{Flag}$-ENaC, with triple-HA, T7, and Flag tags located at the C termini of their respective ENaC subunits, as described in ref. 8, were treated with 10 μM amiloride (a commonly used ENaC inhibitor), 1 μM benzamil (a high specificity ENaC inhibitor), or 100 μM Furin inhibitor 1 for 2 d. Then, cells were lysed in lysis buffer (50 mM Hepes, pH 7.5, 150 mM NaCl, 1% Triton X-100, 10% glycerol, 1.5 mM $MgCl_2$, 1.0 mM ethylene glycol-bis(β-aminoethyl ether)-*N*,*N*,*N*′,*N*-tetra-acetic acid and 10 μg/mL each of leupeptin, aprotinin, and pepstatin, and 1 mM phenylmethanesulfonylfluoride [PMSF]). To detect Nedd4-2 catalytic activity (autoubiquitination), 1 mg of cleared cell lysates was treated with 1% SDS and boiled for 5 min to dissociate protein complexes. Lysates were cooled on ice for 10 min before immunoprecipitation of Nedd4-2 with Flag-agarose and immunoblotting with anti-HA antibodies.

For Nedd4-2 ubiquitination in mouse colonic organoids: Experiments using colonic tissues of killed mice were approved by the Animal Care Committee, The Hospital for Sick Children, Toronto. WT mouse colonic organoids were generated as detailed previously and grown in Matrigel droplets (62). They were then extracted from the Matrigel droplets by 1× TrypLE digestion at 37 °C for 15 min. They were centrifuged and washed once with advanced Dulbecco's modified Eagle's medium (DMEM)/F12. The organoids were then treated in either isotonic NaCl or hypertonic NaCl solutions for 15 min at 37 °C. They were subsequently collected, lysed in lysis buffer, and Nedd4-2 autoubiquitination was detected by immunoprecipitating ubiquitin from the lysates using TUBES agarose and immunoblotting for Nedd4-2.

For binding (coimmunoprecipitation) experiments, ENaC-MDCK cells (8) were induced for 2 d with 1 μM dexamethasone (to induce αENaC expression) and 10 μM sodium butyrate (to enhance the expression of all subunits) and simultaneously treated with 100 μM Furin inhibitor 1 for 2 d. HEK293T cells were transfected with either WT ENaC (V5-tagged αENaC, untagged βENaC, and V5-tagged γENaC ($\alpha_{V5}\beta\gamma_{V5}$-ENaC) or FM ENaC (V5-tagged αR205A/R208A/R231A ENaC, untagged βENaC, and V5-tagged γR143AENaC ($\alpha_{R205A/R208A/R231A\text{-}V5}\beta\gamma_{R143A\text{-}V5}$-ENaC), and Flag-tagged Nedd4-2 (CS) mutant (where indicated). Cells were lysed in lysis buffer as described above and followed by IP of ENaC (with HA-IP in MDCK-ENaC cells or V5-IP in HEK293T cells). Coimmunoprecipitated Nedd4-2 was verified by immunoblotting with Nedd4-2 or Flag antibodies. All immunoblots were imaged using the Odyssey Imaging system (Odssey Fc, LI-COR) and quantified using Image Studio version 3.1.4 (LI-COR).

Nedd4-2 In Vitro Ubiquitination Experiments. Twenty micromoles of purified Nedd4-2 was incubated with 5 μM E1(UBE1), 25 μM E2 (UBE2L3), 3 μM ubiquitin, and 2.5 mM adenosine triphosphate in ubiquitination buffer (50 mM Tris·HCl pH 7.5, 10 mM $MgCl_2$) with increasing concentrations of NaCl (as indicated) for 30 min. The reaction was stopped by boiling in 1× sample buffer. Nedd4-2 catalytic activity was assessed by immunoblotting with anti-ubiquitin antibodies.

Ubiquitination of Cell Surface ENaC. HEK293T cells were seeded in 10-cm dishes coated with poly-D-lysine and transfected with WT ENaC (V5-tagged αENaC, untagged βENaC, and V5-tagged γENaC ($\alpha_{V5}\beta\gamma_{V5}$-ENaC), and either Flag-tagged Nedd4-2 WT or its CS mutant. Where indicated, cells were treated with either 2 μM BIRB796 or 10 μM WNK463 for 2 h. Twenty-four hours posttransfection, cells were washed twice with cold phosphate-buffered saline (PBS) and labeled with 0.5 mg/mL biotin (in cold PBS) for 30 min on ice. Cells were then washed three times with cold PBS containing 25 mM Tris·HCl (pH 7.4) to quench residual biotin, and lysed in lysis buffer. V5-tagged αENaC and V5-tagged γENaC were immunoprecipitated overnight at 4 °C from 4 to 5 mg of lysate using anti-V5 antibodies. Immunoprecipitated total cellular ENaC was washed three times with cold wash buffer (20 mM Hepes pH 7.4, 150 mM NaCl, 1% glycerol, 0.1% Triton X-100) and boiled for 15 min in lysis buffer containing 1% SDS to elute immunoprecipitated ENaC from the Protein G agarose. The supernatant containing both the intracellular ENaC and biotin-labeled surface ENaC fractions was diluted 1:20 with cold lysis buffer to dilute out the SDS, and biotin-labeled surface ENaC was immunoprecipitated using streptavidin agarose at 4 °C for 2 h. The streptavidin beads were washed three times with cold wash buffer and boiled in sample buffer prior to SDS–polyacrylamide gel electrophoresis and immunoblotting.

Ussing Chambers Analysis. MDCK WT cells and ENaC-MDCK cells (described above) were seeded onto Millicell inserts for Ussing chamber assays (short circuit current [Isc] analysis). All cells were incubated in DMEM supplemented with 10% fetal bovine serum plus antibiotics (Pen-Strep), and with additional selection antibiotics (G418, 300 μg/mL; hygromycin, 100 μg/mL; and puromycin,

2 μg/mL), and 10 μM amiloride for the ENaC-MDCK cells. On day 4, ENaC-MDCK cells were induced overnight with 1 μM dexamethasone and 10 μM sodium butyrate. Cells were treated (or not) with 10 μM WNK463 for 2 h prior to mounting on the Ussing chamber (Physiologic Instruments). Once the stable currents were established, 10 μM amiloride was added into the chamber on the apical side to detect ENaC-specific currents. Short circuit current measurements were taken from the points before and after adding amiloride when the currents were stabilized.

ENaC Cell Surface Stability Experiments. ENaC-MDCK cells were induced with 1 μM dexamethasone and 10 μM sodium butyrate for 2 d, or HEK293T cells were transfected either with wild-type ENaC ($\alpha_{V5}\beta\gamma_{V5}$-ENaC) or Flag-Nedd4-2 (CS) mutant, where indicated. Cells were further treated with either 10 μM amiloride (2 d), 2 μM BIRB796 (2 h), or 10 μM WNK463 (or 1 μM or 5 μM, where indicated) for 2 h, before washing with cold PBS and labeling with 0.5 mg/mL biotin (in cold PBS) for 30 min on ice. The cells were washed three times with cold PBS supplemented with 25 mM Tris·HCl pH 7.5 before lysis. Biotin-labeled proteins were immunoprecipitated with streptavidin-agarose and cell surface ENaC was detected by immunoblotting with antibodies against the ENaC subunits.

Measurements of Intracellular Na^+ or K^+ Concentrations. For all intracellular Na^+ ($[Na^+]_i$) and K^+ ($[K^+]_i$) measurements, cells were grown in 6-cm tissue culture plates. HEK293T, FRT, or MDCK cells were treated with either isoosmotic or hyperosmotic solutions (15 min), 40 μM monensin (30 min), or 0.4 M sorbitol (15 min), where indicated. ENaC-MDCK cells were induced as previously described for 2 d in the presence of 10 μM amiloride. HEK293T cells were transfected with ENaC (wild-type and Furin mutant) for 2 d and treated with 10 μM amiloride (2 d) or 10 μg/mL trypsin type 1 (1 h) prior to lysis. Following treatment, the cells were washed three times with an osmotically balanced solution of 150 mM LiCl (300 mOsm) on ice. The cells were lysed overnight at 4 °C in 1% HNO_3. The intracellular Na^+ and K^+ concentrations were measured using a PinAAcle 900F Atomic Absorption Spectrometer (PerkinElmer). The $[Na^+]_i$ concentration was then normalized to cell number and volume, which were determined using a Coulter Counter (Beckman Coulter Multizer 4e).

Cell Imaging. ENaC-MDCK cells were treated with 1 μM dexamethasone and 10 μM sodium butyrate for 2 d to induce ENaC expression. Brightfield images were acquired using a Zeiss Axiovert 200M microscope at 40× magnification. For immunofluorescence experiments, FRT cells were cultured on glass coverslips in six-well plates and subsequently transfected with Flag-Nedd4-2 (WT) using Lipofectamine 3000 reagent. At 24 h posttransfection, cells were treated with either isoosmotic (iso, 310 mOsm) or hyperosmotic (hyper, 580 mOsm) NaCl solution for 15 min at 37 °C. Cells were fixed with 4% paraformaldehyde, permeabilized with 0.1% Triton X-100, and Nedd4-2 was stained by incubation with anti-Flag M2 antibody followed by Alexa Fluor 488 goat anti-mouse secondary antibody. DAPI was used to visualize the nucleus. Coverslips were mounted on microscope slides using Dako mounting medium. Confocal and brightfield images were acquired using a Quorum spinning disk confocal microscope at 60× magnification.

Quantification and Statistical Analysis. All immunoblots were imaged using the Odyssey Imaging system and quantified using Image Studio version 3.1.4 (LI-COR). At least three independent experiments were performed for each analysis. Histogram bars represent mean ± SEM; *P* values: *<0.05; **<0.01; ***<0.001; ****< 0.0001, using unpaired Student *t* test.

Data Availability. All study data are included in the article and/or *SI Appendix*.

ACKNOWLEDGMENTS. We thank Drs. R. Hughey, T. Kleyman, and O. Kashlan (University of Pittsburgh) for the ENaC Furin mutants; E. Hummler (University of Lausanne) for mCCDcl1 cells; and A. Subramanya (University of Pittsburgh) for the WNK1-KO cells. We also acknowledge obtaining reagents from SPARC Drug Discovery, SickKids. This work was supported by a Canadian Institute of Health Research Foundation Grant (FDN-159198) and Cystic Fibrosis Canada Grant (#555377) to D.R.

1. O. Staub *et al.*, WW domains of Nedd4 bind to the proline-rich PY motifs in the epithelial Na+ channel deleted in Liddle's syndrome. *EMBO J.* **15**, 2371–2380 (1996).
2. H. Abriel *et al.*, Defective regulation of the epithelial Na+ channel by Nedd4 in Liddle's syndrome. *J. Clin. Invest.* **103**, 667–673 (1999).
3. V. Kanelis, D. Rotin, J. D. Forman-Kay, Solution structure of a Nedd4 WW domain-ENaC peptide complex. *Nat. Struct. Biol.* **8**, 407–412 (2001).
4. V. Kanelis, M. C. Bruce, N. R. Skrynnikov, D. Rotin, J. D. Forman-Kay, Structural determinants for high-affinity binding in a Nedd4 WW3* domain-Comm PY motif complex. *Structure* **14**, 543–553 (2006).
5. E. Kamynina, C. Debonneville, M. Bens, A. Vandewalle, O. Staub, A novel mouse Nedd4 protein suppresses the activity of the epithelial Na+ channel. *FASEB J.* **15**, 204–214 (2001).
6. K. F. Harvey, A. Dinudom, D. I. Cook, S. Kumar, The Nedd4-like protein KIAA0439 is a potential regulator of the epithelial sodium channel. *J. Biol. Chem.* **276**, 8597–8601 (2001).
7. R. Zhou, S. V. Patel, P. M. Snyder, Nedd4-2 catalyzes ubiquitination and degradation of cell surface ENaC. *J. Biol. Chem.* **282**, 20207–20212 (2007).
8. C. Lu, S. Pribanic, A. Debonneville, C. Jiang, D. Rotin, The PY motif of ENaC, mutated in Liddle syndrome, regulates channel internalization, sorting and mobilization from subapical pool. *Traffic* **8**, 1246–1264 (2007).
9. A. Escobedo *et al.*, Structural basis of the activation and degradation mechanisms of the E3 ubiquitin ligase Nedd4L. *Structure* **22**, 1446–1457 (2014).
10. A. Persaud *et al.*, Tyrosine phosphorylation of NEDD4 activates its ubiquitin ligase activity. *Sci. Signal.* **7**, ra95 (2014).
11. J. Wang *et al.*, Calcium activates Nedd4 E3 ubiquitin ligases by releasing the C2 domain-mediated auto-inhibition. *J. Biol. Chem.* **285**, 12279–12288 (2010).
12. I. Attali *et al.*, Ubiquitylation-dependent oligomerization regulates activity of Nedd4 ligases. *EMBO J.* **36**, 425–440 (2017).
13. C. Ronzaud *et al.*, Renal tubular NEDD4-2 deficiency causes NCC-mediated salt-dependent hypertension. *J. Clin. Invest.* **123**, 657–665 (2013).
14. C. Jiang, H. Kawabe, D. Rotin, The ubiquitin ligase Nedd4L regulates the Na/K/2Cl co-transporter NKCC1/SLC12A2 in the colon. *J. Biol. Chem.* **292**, 3137–3145 (2017).
15. C. M. Canessa, J. D. Horisberger, B. C. Rossier, Epithelial sodium channel related to proteins involved in neurodegeneration. *Nature* **361**, 467–470 (1993).
16. C. M. Canessa *et al.*, Amiloride-sensitive epithelial Na+ channel is made of three homologous subunits. *Nature* **367**, 463–467 (1994).
17. B. C. Rossier, S. Pradervand, L. Schild, E. Hummler, Epithelial sodium channel and the control of sodium balance: Interaction between genetic and environmental factors. *Annu. Rev. Physiol.* **64**, 877–897 (2002).
18. D. Rotin, O. Staub, Function and regulation of the epithelial Na^+ channel ENaC. *Compr. Physiol.* **11**, 2017–2045 (2021).
19. C. Planès *et al.*, ENaC-mediated alveolar fluid clearance and lung fluid balance depend on the channel-activating protease 1. *EMBO Mol. Med.* **2**, 26–37 (2010).
20. S. Malsure *et al.*, Colon-specific deletion of epithelial sodium channel causes sodium loss and aldosterone resistance. *J. Am. Soc. Nephrol.* **25**, 1453–1464 (2014).
21. S. Noreng, A. Bharadwaj, R. Posert, C. Yoshioka, I. Baconguis, Structure of the human epithelial sodium channel by cryo-electron microscopy. *eLife* **7**, e39340 (2018).
22. S. Noreng, R. Posert, A. Bharadwaj, A. Houser, I. Baconguis, Molecular principles of assembly, activation, and inhibition in epithelial sodium channel. *eLife* **9**, e59038 (2020).
23. T. R. Kleyman, M. D. Carattino, R. P. Hughey, ENaC at the cutting edge: Regulation of epithelial sodium channels by proteases. *J. Biol. Chem.* **284**, 20447–20451 (2009).
24. L. Schild *et al.*, Identification of a PY motif in the epithelial Na channel subunits as a target sequence for mutations causing channel activation found in Liddle syndrome. *EMBO J.* **15**, 2381–2387 (1996).
25. H. Tamura *et al.*, Liddle disease caused by a missense mutation of beta subunit of the epithelial sodium channel gene. *J. Clin. Invest.* **97**, 1780–1784 (1996).
26. R. P. Lifton, A. G. Gharavi, D. S. Geller, Molecular mechanisms of human hypertension. *Cell* **104**, 545–556 (2001).
27. O. Staub *et al.*, Regulation of stability and function of the epithelial Na+ channel (ENaC) by ubiquitination. *EMBO J.* **16**, 6325–6336 (1997).
28. M. B. Butterworth *et al.*, Rab11b regulates the trafficking and recycling of the epithelial sodium channel (ENaC). *Am. J. Physiol. Renal Physiol.* **302**, F581–F590 (2012).
29. T. R. Kleyman, D. C. Eaton, Regulating ENaC's gate. *Am. J. Physiol. Cell Physiol.* **318**, C150–C162 (2020).
30. S. Sheng, M. D. Carattino, J. B. Bruns, R. P. Hughey, T. R. Kleyman, Furin cleavage activates the epithelial Na+ channel by relieving Na+ self-inhibition. *Am. J. Physiol. Renal Physiol.* **290**, F1488–F1496 (2006).
31. M. D. Carattino *et al.*, The epithelial Na+ channel is inhibited by a peptide derived from proteolytic processing of its alpha subunit. *J. Biol. Chem.* **281**, 18901–18907 (2006).
32. J. B. Bruns *et al.*, Epithelial Na+ channels are fully activated by furin- and prostasin-dependent release of an inhibitory peptide from the gamma-subunit. *J. Biol. Chem.* **282**, 6153–6160 (2007).
33. M. D. Carattino *et al.*, Defining an inhibitory domain in the alpha-subunit of the epithelial sodium channel. *Am. J. Physiol. Renal Physiol.* **294**, F47–F52 (2008).
34. C. J. Passero *et al.*, Defining an inhibitory domain in the gamma subunit of the epithelial sodium channel. *Am. J. Physiol. Renal Physiol.* **299**, F854–F861 (2010).
35. O. B. Kashlan *et al.*, Allosteric inhibition of the epithelial Na+ channel through peptide binding at peripheral finger and thumb domains. *J. Biol. Chem.* **285**, 35216–35223 (2010).
36. O. B. Kashlan, B. M. Blobner, Z. Zuzek, M. D. Carattino, T. R. Kleyman, Inhibitory tract traps the epithelial Na+ channel in a low activity conformation. *J. Biol. Chem.* **287**, 20720–20726 (2012).
37. R. Kabra, K. K. Knight, R. Zhou, P. M. Snyder, Nedd4-2 induces endocytosis and degradation of proteolytically cleaved epithelial Na+ channels. *J. Biol. Chem.* **283**, 6033–6039 (2008).
38. G. Frindt, M. Bertog, C. Korbmacher, L. G. Palmer, Ubiquitination of renal ENaC subunits in vivo. *Am. J. Physiol. Renal Physiol.* **318**, F1113–F1121 (2020).
39. R. P. Hughey *et al.*, Epithelial sodium channels are activated by furin-dependent proteolysis. *J. Biol. Chem.* **279**, 18111–18114 (2004).
40. R. P. Hughey *et al.*, Maturation of the epithelial Na+ channel involves proteolytic processing of the alpha- and gamma-subunits. *J. Biol. Chem.* **278**, 37073–37082 (2003).

41. A. Chraïbi, V. Vallet, D. Firsov, S. K. Hess, J. D. Horisberger, Protease modulation of the activity of the epithelial sodium channel expressed in Xenopus oocytes. *J. Gen. Physiol.* **111**, 127–138 (1998).
42. J. G. Bode *et al.*, The mitogen-activated protein (MAP) kinase p38 and its upstream activator MAP kinase kinase 6 are involved in the activation of signal transducer and activator of transcription by hyperosmolarity. *J. Biol. Chem.* **274**, 30222–30227 (1999).
43. V. N. Bildin, Z. Wang, P. Iserovich, P. S. Reinach, Hypertonicity-induced p38MAPK activation elicits recovery of corneal epithelial cell volume and layer integrity. *J. Membr. Biol.* **193**, 1–13 (2003).
44. P. de Los Heros, D. Pacheco-Alvarez, G. Gamba, Role of WNK kinases in the modulation of cell volume. *Curr. Top. Membr.* **81**, 207–235 (2018).
45. A. Roy *et al.*, Generation of WNK1 knockout cell lines by CRISPR/Cas-mediated genome editing. *Am. J. Physiol. Renal Physiol.* **308**, F366–F376 (2015).
46. J. Han, J. D. Lee, L. Bibbs, R. J. Ulevitch, A MAP kinase targeted by endotoxin and hyperosmolarity in mammalian cells. *Science* **265**, 808–811 (1994).
47. T. Moriguchi *et al.*, Purification and identification of a major activator for p38 from osmotically shocked cells. Activation of mitogen-activated protein kinase kinase 6 by osmotic shock, tumor necrosis factor-alpha, and H2O2. *J. Biol. Chem.* **271**, 26981–26988 (1996).
48. C. Debonneville *et al.*, Phosphorylation of Nedd4-2 by Sgk1 regulates epithelial Na(+) channel cell surface expression. *EMBO J.* **20**, 7052–7059 (2001).
49. P. M. Snyder, D. R. Olson, R. Kabra, R. Zhou, J. C. Steines, cAMP and serum and glucocorticoid-inducible kinase (SGK) regulate the epithelial Na(+) channel through convergent phosphorylation of Nedd4-2. *J. Biol. Chem.* **279**, 45753–45758 (2004).
50. V. Bhalla *et al.*, Serum- and glucocorticoid-regulated kinase 1 regulates ubiquitin ligase neural precursor cell-expressed, developmentally down-regulated protein 4-2 by inducing interaction with 14-3-3. *Mol. Endocrinol.* **19**, 3073–3084 (2005).
51. H. Abriel, J. D. Horisberger, Feedback inhibition of rat amiloride-sensitive epithelial sodium channels expressed in Xenopus laevis oocytes. *J. Physiol.* **516**, 31–43 (1999).
52. M. B. Butterworth *et al.*, The deubiquitinating enzyme UCH-L3 regulates the apical membrane recycling of the epithelial sodium channel. *J. Biol. Chem.* **282**, 37885–37893 (2007).
53. D. Ruffieux-Daidié *et al.*, Deubiquitylation regulates activation and proteolytic cleavage of ENaC. *J. Am. Soc. Nephrol.* **19**, 2170–2180 (2008).
54. R. Zhou *et al.*, Ubiquitin-specific peptidase 8 (USP8) regulates endosomal trafficking of the epithelial Na+ channel. *J. Biol. Chem.* **288**, 5389–5397 (2013).
55. D. Lagnaz *et al.*, WNK3 abrogates the NEDD4-2-mediated inhibition of the renal Na+-Cl- cotransporter. *Am. J. Physiol. Renal Physiol.* **307**, F275–F286 (2014).
56. S. Shibata, J. Zhang, J. Puthumana, K. L. Stone, R. P. Lifton, Kelch-like 3 and cullin 3 regulate electrolyte homeostasis via ubiquitination and degradation of WNK4. *Proc. Natl. Acad. Sci. U.S.A.* **110**, 7838–7843 (2013).
57. L. M. Boyden *et al.*, Mutations in kelch-like 3 and cullin 3 cause hypertension and electrolyte abnormalities. *Nature* **482**, 98–102 (2012).
58. T. Kimura *et al.*, Deletion of the ubiquitin ligase Nedd4L in lung epithelia causes cystic fibrosis-like disease. *Proc. Natl. Acad. Sci. U.S.A.* **108**, 3216–3221 (2011).
59. P. P. Shi *et al.*, Salt-sensitive hypertension and cardiac hypertrophy in mice deficient in the ubiquitin ligase Nedd4-2. *Am. J. Physiol. Renal Physiol.* **295**, F462–F470 (2008).
60. E. Heidrich *et al.*, Intracellular Na+ regulates epithelial Na+ channel maturation. *J. Biol. Chem.* **290**, 11569–11577 (2015).
61. S. Wiesner *et al.*, Autoinhibition of the HECT-type ubiquitin ligase Smurf2 through its C2 domain. *Cell* **130**, 651–662 (2007).
62. W. L. Demian *et al.*, The ion transporter NKCC1 links cell volume to cell mass regulation by suppressing mTORC1. *Cell Rep.* **27**, 1886–1896.e1886 (2019).